LAWRENCE
LIVERMORE
NATIONAL
LABORATORY

LLNL-JRNL-416502

Limitation on Pre-pulse Level for Cone-Guided Fast-Ignition ICF

A. G. MacPhee, K. U. Akli, F. N. Beg, C. D. Chen, H. Chen, L. Divol, D. S. Hey, R. R. Freeman, M. Henesian, A. J. Kemp, M. H. Key, S. Le Pape, A. Link, T. Ma, A. J. Mackinnon, V. M. Ovchinnikov, P. K. Patel, T. W. Phillips, R. B. Stephens, M. Tabak, R. Town, L. D. Van Woerkom, M. S. Wei, S. C. Wilks

September 2, 2009

Physical Review Letters

Disclaimer

Limitation on Pre-pulse Level For Cone-Guided Fast-Ignition ICF

A. G. MacPhee[1], K. U. Akli[2], F. N. Beg[3], C. D. Chen[1], H. Chen[1], L. Divol[1], D. S. Hey[1], R. R. Freeman[4], M. Henesian[1], A. J. Kemp[1], M. H. Key[1], S. Le Pape[1], A. Link[4], T. Ma[1,3], A. J. Mackinnon[1], V. M. Ovchinnikov[4], P. K. Patel[1], T. W. Phillips[1], R. B. Stephens[2], M. Tabak[1], R. Town[1], L. D. Van Woerkom[4], M. S. Wei[3], S.C. Wilks[1]

[1]*Lawrence Livermore National Laboratory, Livermore, CA*
[2]*General Atomics, San Diego, CA*
[3]*Department of Mechanical and Aerospace Engineering, University of California-San Diego, La Jolla, CA*
[4]*College of Mathematical and Physical Sciences, The Ohio State University, Columbus, OH*
(925) 422 3720, macphee2@llnl.gov

Abstract. The viability of fast-ignition (FI) inertial confinement fusion hinges on the efficient transfer of laser energy to the compressed fuel via multi-MeV electrons. Pre-formed plasma due to laser pre-pulse strongly influences ultra-intense laser plasma interactions and hot electron generation in the hollow cone of an FI target. We induced a prepulse and consequent preplasma in copper cone targets and measured the energy deposition zone of the main pulse by imaging the emitted K_α radiation. An integrated simulation of radiation hydrodynamics for the pre-plasma and particle in cell for the main pulse interactions agree well with the measured deposition zones and provide an insight into the enrgy deposition mechanism and electron distribution. It was demonstrated that a under these conditions a 100mJ pre-pulse completely eliminates the forward going component of ~2-4MeV electrons. Consequences for cone-guided fast-ignition are discussed.

Keywords: Fast Ignition, Inertial Confinement Fusion, ICF, PIC.
PACS: 52.50.Jm, 52.38.Hb, 52.38.Kd, 52.38.Mf, 52.70.La, 52.57.Kk

Cone-guided fast ignition inertial confinement fusion (FI) depends on the efficient transfer of laser energy to a forward directed beam of ~2MeV electrons at the tip of a hollow cone embedded in the side of an ICF fuel capsule [i]. This scheme is particularly susceptible to laser pre-pulse [ii,iii] as the cone wall confines the expanding pre-formed plasma [iv,v] increasing both density scale lengths and laser beam filamentation [vi].

The igniter laser pulse requirements for fast ignition depend on the conversion efficiency from laser energy to hot electrons [vii], the electron energy spectrum [viii], the electron transport efficiency to the ignition hot spot [ix,x] and the electron energy deposition efficiency in the hot spot [x]. The required laser energy has been estimated at approximately 100kJ in a 20 ps pulse [i,xi]. Since the ignition hot spot diameter is ~40μm, the cone tip must be similar in diameter and the laser intensity ~$4x10^{20}$W/cm^2. Existing petawatt class laser systems with OPCPA front ends deliver up to 1kJ with typical ASE energy contrast ~$1x10^{-5}$ and with non linear devices this ratio can be reduced by a further order of magnitude [xii]. As contrast is independent of laser energy at FI scale of 100kJ, the pre-pulse energy on target could range from 100 mJ to 1J. Recent work by Baton et al., [v] has shown that some amount of pre-pulse can strongly affect coupling to cones however a detailed understanding of this limit has not been reported.

In this letter we report recent studies of laser interactions with hollow cone targets comparing simulations and experiments in conditions approaching full FI using pre-pulse up to 100mJ with main pulse irradiance ~10^{20}Wcm^{-2} for picosecond durations. These perameters were accessible using the Titan laser at LLNL, which delivers (150±10)J in (0.7+/-0.2)ps, with ~10% of the energy deposited above an intensity of ~10^{20}Wcm^{-2} at best focus [xiii].

We compare coupling for two well characterized pre-pulse conditions: 1) an intrinsic Titan laser pre-pulse with (7.5±3)mJ in 1.7ns at 7.5x10^{10}Wcm^{-2} and 2) (100±3)mJ, 3.0ns pre-pulse at ~10^{12}Wcm^{-2}. The larger pre-pulse was generated by injecting an auxiliary laser pulse into the short pulse amplifier chain prior to the main pulse. Targets were 1mm long copper cones with 30° co-angle, 25μm wall thickness and 30μm internal tip diameter. The energy distribution for the intrinsic pre-pulse, the auxiliary pre-pulse and the main pulse were measured by sampling beam leakage through the last turning mirror prior to the final focusing optic, at a plane equivalent to the focal plane on target [xiii]. Best focus for both the pre-pulse and the main pulse was set at the inside surface of the cone tip.

The system was modeled in two parts: i) The radiative-hydro code HYDRA [xiv] was used to calculate the distribution of the preformed plasma created by laser ablation from the inside wall of the cone due to the pre-pulse. ii) The plasma simulation code PCS [xv] was used to perform a massively parallel particle in cell (PIC) simulation of the ultra-intense short pulse laser interaction with the preformed plasma and to calculate the distribution of hot electrons as a function of time. The two-dimensional PIC simulations of the laser-cone interactions were all performed at full spatial and temporal scales. 20 cells per wavelength and 50 particles per cell were used. The density of the cone wall was clamped at 100x critical (n_c) to avoid numerical heating. The initial conditions for the PIC simulation were imported from a 2D hydrodynamic simulation performed using the fluid code HYDRA [xiv], using the as-shot target geometry and the as-measured pre-pulse (both intrinsic and external). The near field intensity distribution of the Titan laser was reconstructed from the measured high power focal spot, resulting in an aberrated spot consistent with experiment. This near field was used as a boundary condition for the Maxwell solver in the PIC simulation. In order to capture the correct pre-plasma evolution, the PIC simulation was started at 3% of peak laser power, 1ps before the peak. Significant channel pre-formation was observed during the first picosecond, which was able to subsequently guide the laser light near peak power. It should be noted that using a realistic focal spot, pre-plasma and starting the simulation at very low power lead to significant differences compared to an ideal simulation (Gaussian spot simulated for a FWHM) in terms of channel formation and energy deposition.

In the experiment the time integrated distribution of K_α fluorescence radiation from copper cone targets was measured using a spherically bent quartz crystal X-ray microscope tuned to Cu K_α radiation at 8027.8eV with ~5.2eV bandwidth [xvi,xvii] and a magnification of x7 as shown in figure 1. Under these conditions the dominant excitation of K_α is from binary collisions with the hot electrons, hence the Cu K-shell emission correlates closely with the distribution of hot electrons [iv,xviii].

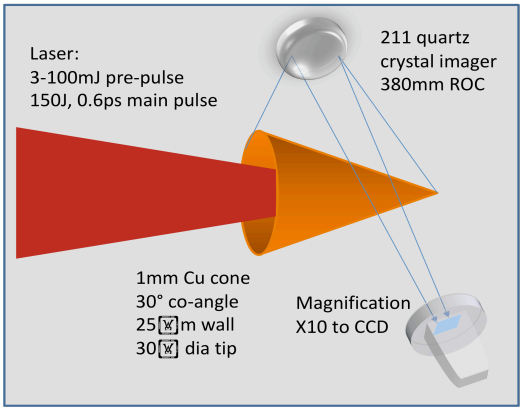

FIGURE 1. Target detail illustrating K_α imaging geometry.

As shown in previous work [xvii] there is direct correspondence between the measured K_α at a given point in the image and the calculated hot electron density. The energy lost per K_α event is small compared to the average energy of the hot electrons; hence the summation can be performed over the electron distribution alone, neglecting losses due to K_α production and significantly simplifying the calculation.

The Cu K_α images are shown in figure 2a. The lower and upper parts of the figure are data from Cu cone targets irradiated using the Titan laser as described above, with the 7.5mJ and 100mJ pre-pulse

respectively. There are clear and striking differences between the low and high pre-pulse case as illustrated by the on-axis line-outs superimposed on the image.

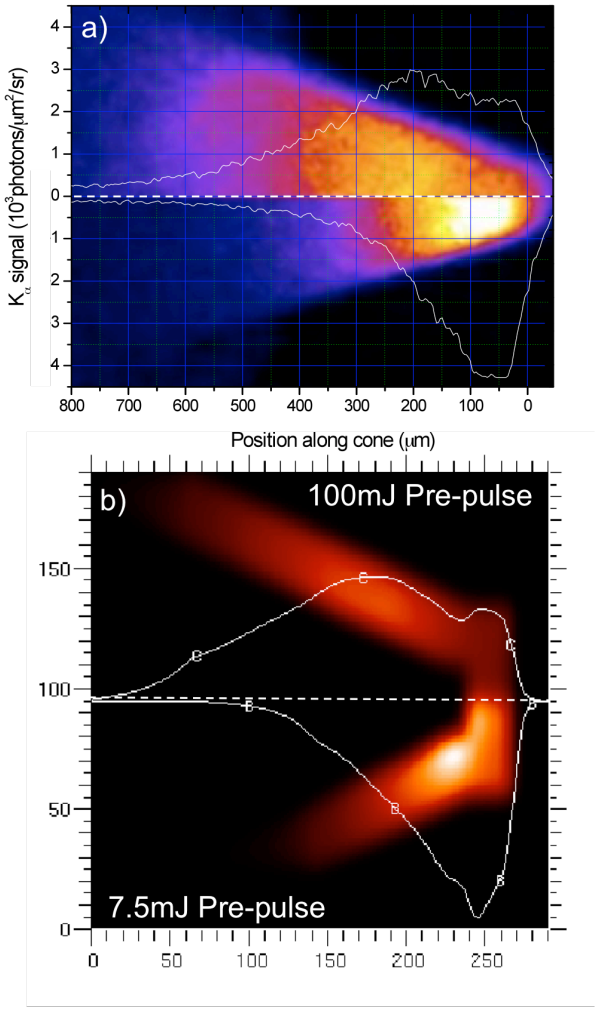

FIGURE 2. a) Time integrated K_α signal. b) Time integrated K_α from model. White curves are transverse integration. Upper: 100mJ pre-pulse, lower: 7.5mJ pre-pulse.

First for the 7.5mJ pre-pulse the K_α emission rises sharply, with a well defined peak 50μm from tip, before decreasing rapidly over the next 200μm. For the 100mJ pre-pulse case the distribution is much more broadly distributed 200μm from the cone tip and extending for a further 500μm along the cone. These data are completely consistent with pre-plasma filling within the cone forcing the hot electron source further down the cone.

Direct comparison with the PIC/HYDRO modeling allows more insight into this process. The electron distributions from the PIC simulations were post-processed to compute the time integrated K_α emission over the 3 ps simulated by integrating over the electron energy distribution function and the electron cross section for K_α production. Figure 2b shows the resulting K_α deposition zones where $\iint n_e(E)\, \sigma_{K\alpha}(E)\, n_{ion}$ dvdt (was calculated from particle dumps every 70 fs. The simulations reproduce the essential points from the experimental data; with a well defined peak 30-50μm from the cone tip for the low pre-pulse case and a broad distribution centered at 150microns for the 100mJ pre-pulse.

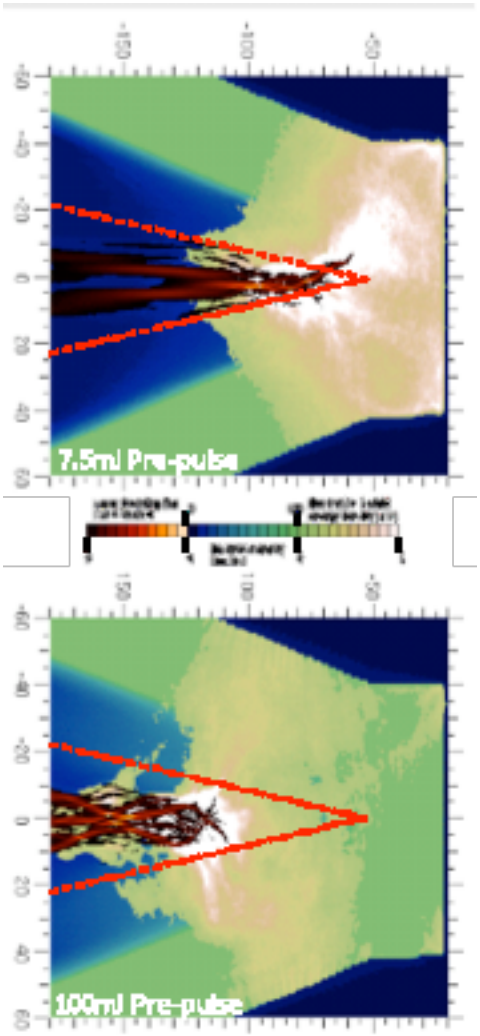

FIGURE 3. Overlay of laser Poynting flux and electron density map 1ps after nominal peak fluence on target: a) 7.5mJ pre-pulse b) 100mJ pre-pulse.

The origin of these features is clear from examination of the laser interaction with the preformed plasma using the PCS PIC simulations as shown in figure 3. Here the laser Poynting flux is plotted at the

time of peak main pulse fluence for both cases up to 4×10^{20}Wcm^{-2} using a red color ramp. The pre-formed plasma used as the starting conditions for the PIC simulation is illustrated using a blue-green ramp representing electron density up to $100n_c$. The hot electron energy density above 1MeV normalized to 1 at the end of the three ps simulation is illustrated using the green-white color ramp. In the 7.5mJ case the critical density surface on axis is 10μm from the inside tip of the cone. Rapid filamentation and self-focusing compared to the geometric focus (red dash) become apparent in the pre-formed plasma ~60μm from the tip. In the 100mJ pre-pulse case the critical density surface on axis is promoted an additional 30microns from the tip and self-focusing switches on at ~120μm. Best focus has an envelope approximately twice the initial diameter and has shifted an additional ~30μm upstream.

Multiple effects explain the quantitative differences: First, we did not account for transport effects over tens of picoseconds, where multi-MeV electrons will spray K_α emission over their mean-free path which is ~1mm in Cu. This will likely extend the scale length of the K_α emission towards the back of the cone. This would not significantly change the relative contrast between the cone tip and the wall, as the K_α bright spots in figure 2 are dominated by 100-300 keV electrons that have < 100μm mean-free-path. Second, we expect self-focusing in 3D to be stronger than that observed in the 2D simulation, which would promote the filamentation zone further from the cone tip, most significantly for the 100mJ case.

For an f/3, 1μm laser beam at peak intensity ~$2x10^{20}$Wcm^{-2}, all of the laser energy is diverted from the cone tip by the pre-formed plasma associated with a ~100mJ pre-pulse. The dynamics of relativistic filamentation lead to a very different picture depending on the pre-plasma scalelength. In the 7mJ pre-pulse case, one main filament is able to bore a hole through the short pre-plasma and reach the tip of the cone (albeit slightly off-axis). With 100mJ of imposed pre-pulse, the laser beam splits into multiple filaments far from best focus (and the tip of the cone), its propagation is halted and energetic electrons are generated mostly sideways. Figure 3 illustrates that these simulated images are in good qualitative agreement with the experiment.

The scale, duration and resolution of the PIC simulation, along with the inclusion of beam filamentation and the radiative-hydro simulation of the initial pre-formed plasma is a significant step towards a fully integrated model of laser plasma interactions for fast ignition cone targets.

ACKNOWLEDGEMENTS

This work performed under the auspices of the U.S. Department of Energy by Lawrence Livermore National Laboratory under Contract DE-AC52-07NA27344.

REFERENCES

i M. Tabak, *et al*., Phys. Plasmas **1**, 1626 (1994)
ii K.B. Wharton *et al*., Phys. Rev. E. **64** 025401 (2001)
iii F Tavella et al., New J. Phys. **8** 219 (2006)
iv L. Van Woerkom *et al*., Phys. Plasmas **15**(5) 056304 (2008)
v S.D. Baton *et al.*, Phys. Plasmas **15**(4), 042706 (2008)
vi N. Kumar *et al*., Phys. Scr. **73,** 659–662 (2006) and references therein.
vii M.H. Key *et al*., Phys. Plasmas **5**, 1966 (1998); A. L. Lei *et al*., Phys. Rev. Lett. **96**, 255006 (2006)
C.D. Chen, *et al*., Phys. Plasmas **16,** 082705 (2009)
ix M. Roth *et al*., Laser and Particle Beams **23** (1), 95-100 (2004)
x J.J. Honrubia *et al*., Nucl. Fusion **46**, L25-L28 (2006)
xi S. Atzeni, Phys. Plasmas **14**, 052702 (2007)
xii A Cotel *et al*., Appl. Phys. B **83** 7 (2006); A. Jullian *et al*., Opt. Lett. **30**(8), 920 (2005)
xiii A.G. MacPhee *et al*., Rev. Sci. Instrum. **79**(10), 10F302 (2008)
xiv M. Marinak *et al*., Phys. Plasmas **5**, 1125 (1998)
xv H. Ruhl, M. *et al*., in "Introduction to Computational Methods in Many Particle Body Physics" (Rinton, Paramus, New Jersey, 2006); M. Bonitz, *et* al., "Introduction to Computational Methods in Many Body Physics" (Cambridge University Press, Cambridge, England, 2004); H. Ruhl, "Collective Super-Intense Laser-Plasma Interaction", Habilitationsschrift, Technische Universität Darmstadt (2000)
xvi J. A. Koch , Rev. Sci. Instrum. **74**, 2130 (2003)
xvii R.B. Stephens *et al*., Phys. Rev. E **69**, 066414 (2004)
xviii Ch. Reich *et al*., Phys. Rev. Lett. **84**(21) 4846 (2000)